A cobalt-rich spinel inclusion in a sapphire from Bo Ploi, Thailand

JINGFENG GUO*, W. L. GRIFFIN+ AND S. Y. O'REILLY*

* School of Earth Sciences, Macquarie University, NSW 2109, Australia
+ CSIRO Division of Exploration Geoscience, P.O. Box 136, North Ryde, NSW 2113, Australia

Abstract

Cobalt-rich spinel is found as a ~200 μm inclusion, together with a glassy phase, in a gem-quality blue sapphire from Bo Ploi, Thailand. This is the first reported natural occurrence of such a spinel. Its composition is directly analogous with that of cochromite, a previously reported rare cobalt-rich chromite. The compositional ranges for the cobalt-rich spinel, obtained using electron microprobe and proton microprobe (methods described below), are Al_2O_3 48.18–61.27 %, CoO 19.7–22.84 %, Cr_2O_3 0–12.28 %, FeO 8.64–9.67 %, MgO 6.04–6.89, TiO_2 0.49–0.73 %, Ni 2251–2532 p.p.m., Zn 335–371 p.p.m., Mn < 177–849 p.p.m., Ga 113–153 p.p.m., Nb 24–1252 p.p.m., Zr < 4–167 p.p.m., Sn 22–428 p.p.m., As < 4–56 p.p.m., Sr < 4–59 p.p.m., Ag 13–64 p.p.m. Transition elements decrease in abundance from core to rim of the spinel while the other elements increase. Crystal chemical considerations suggest that a vacancy-creating substitution mechanism may be operative in the cobalt-rich spinel despite the small scale, i.e. $3Co^{2+} = 2Al^{3+} + {}^{[4]}\square$. The glassy phase coexisting with the spinel is likely to be the product of heating by the host basaltic magma. The mode of occurrence of the cobalt-rich spinel prevents further physical investigation. This unusual spinel is considered to be the result of a complex magma mixing process in the lower crust.

KEYWORDS: cobalt, spinel, corundum, sapphire, megacryst, alkali basalt, Thailand

Introduction

INCLUSIONS of one mineral in another reveal valuable information about the physical and chemical environment of the host mineral at the time of its formation. This is particularly important for the study of gemstones, which are often found in geological contexts that tell little about their origin, e.g. in alluvial deposits or as xenocrysts in volcanic rocks. Earlier investigations of gem-quality corundum (sapphire and ruby) have shown that a wide spectrum of mineral phases (over 30 species) are present as inclusions but each gem-field tends to give different inclusion combinations (Gübelin and Koivula, 1986). The mineral paragenesis and the chronological relationship between individual minerals in principle could be used to identify the source characteristics and the processes involved in the generation of the host sapphires. As part of a project on the genesis of sapphire, a recent study of the mineral inclusions within sapphires from various fields has yielded important new information. This paper reports the occurrence of a spinel inclusion with a unique composition — a cobalt-rich spinel.

Geological background

Bo Ploi is located approximately 40 km north of Kanchanaburi, about 130 km to the west of Bangkok, Thailand (Fig. 1). Sapphires are recovered nearly exclusively from the alluvial/eluvial deposits near basaltic outcrops in the vicinity of Bo Ploi and the mining is concentrated on the so-called 'gem-bearing gravels' which lie a few m below the surface (Vichit *et al.*, 1978). Some sapphires were reportedly obtained from residual soils overlying basaltic rocks (Bunopas and Bunjitradulya, 1975). At present the Bo Ploi mines are Thailand's major producer of sapphire; this is mainly blue, but occasionally yellow and pink.

Due to the tropical climate of the region, most rocks have been heavily weathered, forming an extensive coverage of soils and vegetation. However, detailed studies on the alkalic basaltic

Mineralogical Magazine, June 1994, Vol. 58, pp. 247–258

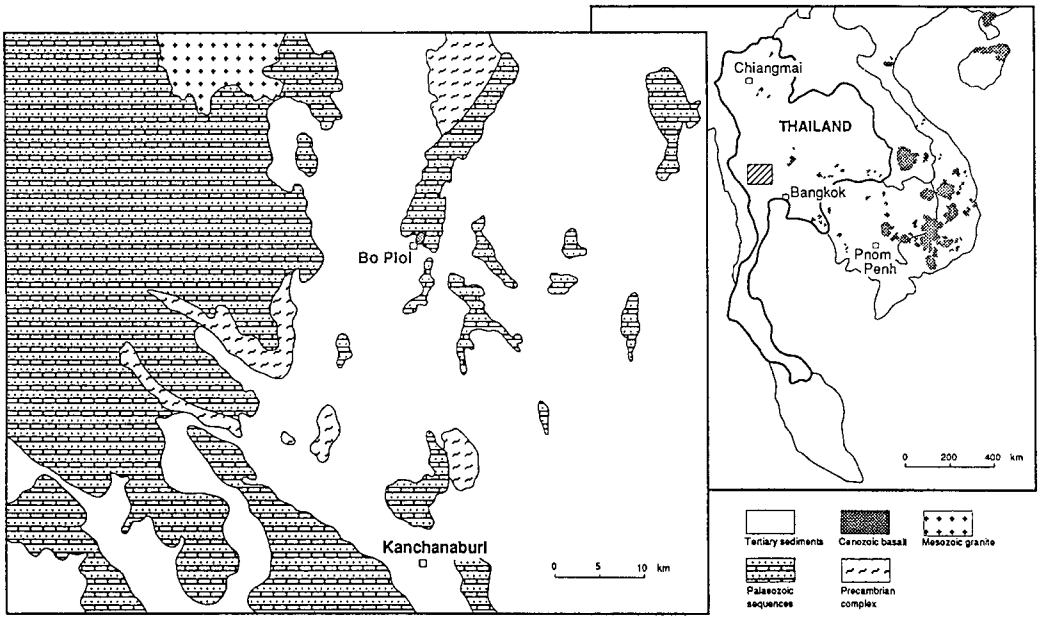

FIG. 1. The geological map of Bo Ploi area, Thailand (Simplified after Vichit *et al.*, 1978). The attached map shows the distribution of Cenozoic basaltic rocks throughout the Southeast Asian region.

rocks of Thailand have been carried out and yielded significant amounts of information (e.g. Barr and MacDonald, 1978, 1979; Vichit *et al.*, 1978). According to Barr and MacDonald (1978), nepheline hawaiite is the only type of basaltic rock around Bo Ploi and the erosion in this area has been so severe that nepheline hawaiite remains only as a semicircular plug 300 m in diameter, representing the old volcanic eruption centre. The hawaiitic plug contains abundant spinel lherzolite xenoliths and megacrysts; the most common megacrysts are black clinopyroxene, spinel, nepheline, plagioclase, sanidine and anorthoclase. Although the nepheline hawaiite of Bo Ploi was not dated, it was estimated to be younger than 3 Ma, belonging to the large Cenozoic Southeast Asia volcanic province (Barr and MacDonald, 1981). Direct observations of sapphire *in situ* are generally rare, but the presence of sapphire in basaltic rocks at Bo Ploi has been reported as 'quite usual' compared with other sapphire fields in Thailand (Gunawardene and Chawla, 1984).

The basement rocks in the area of Bo Ploi range from Precambrian marble and gneiss complexes to the Palaeozoic sedimentary succession intruded by granitic bodies of Cretaceous to Triassic age, and minor Mesozoic sedimentary sequences (Fig. 1); (Bunopas and Bunjitadulya, 1975). The Precambrian complexes are interbedded metasedimentary sequences affected by an upper amphibolite facies metamorphism. The mineral assemblages of the gneisses include microcline, tremolite, plagioclase, quartz, biotite, muscovite, apatite and zircon. The massive marbles contain accessories such as muscovite and tremolite. The Palaeozoic sedimentary succession is composed of limestone, sandstone, phyllite, shale and locally quarzite, and is overlain by minor Mesozoic sediments of similar lithology. Gravels and sandy alluvium were widely developed since Tertiary time.

Sample descriptions

In this study, more than 20 individual sapphire fragments were selected and optically examined for inclusions. Sample BP8, in which an unusual inclusion was found, is a parti-coloured greenish blue stone with no fractures. The inclusion is an elongated multiphase assemblage (composite inclusion). The central portion is a dark Co- and Al-rich phase surrounded by a relatively softer yellowish brown material that appears to be homogeneous and glassy (Fig. 2). A number of small euhedral crystals of the Co,Al-rich phase are distributed at both ends of the elongated inclusion

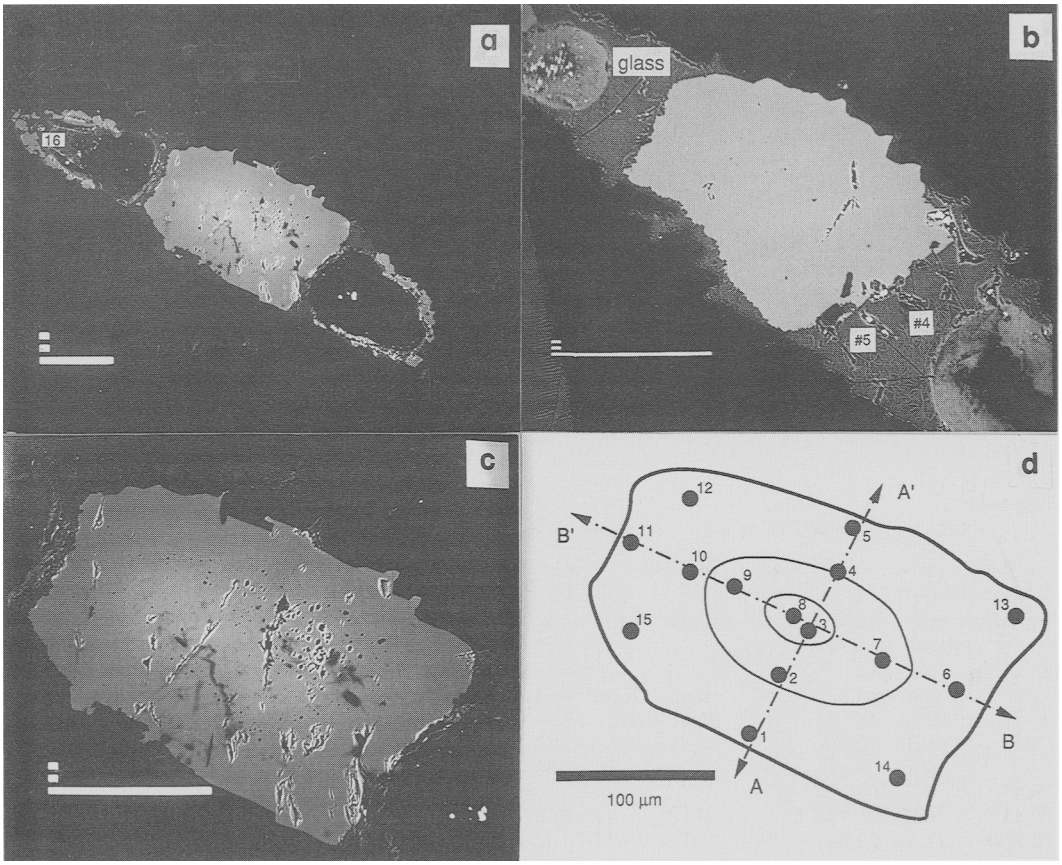

FIG. 2. Backscattered electron images of cobalt-rich spinel in sapphire. (*a*) The entire composite inclusion with a length of 0.6 mm (Some material was rubbed off at both ends of the assemblage during the grinding-polishing process). (*b*) A section 20 μm deeper than (*a*). Numbers indicate the glass areas analysed by electron microprobe. (*c*) Close-up of the large cobalt-rich spinel grain. The gradual change of contrast from centre to margin reflects the compositional variation of spinel, principally Cr and Al. (*d*) Sketch map of (*c*) showing the actual positions of EMP analyses (see Table 1 for data).

in contact with the host corundum. Under transmitted light, the Co- and Al-rich inclusions are dark but transparent and isotropic, exhibiting a deep blue colour near the edge of the grain. The largest grain is approximately 250 μm × 150 μm. Apart from this composite inclusion in grain BP8, albite was found in this study to be a common type of inclusion in Bo Ploi sapphires. Other investigations on sapphires from Bo Ploi have identified inclusions of K-feldspar, Na-Mg-Al amphibole and pyrrhotite (Gunawardene and Chawla, 1984). It must be mentioned that we cannot confirm whether the sapphire samples used in the present investigation have been heat-treated. However, judging from the lack of obvious fractures throughout the sample BP8, and the characteristic element zoning of the large crystal, we infer that there has been no heat treatment and that the cobalt-rich spinel is a mineral formed by natural processes.

Analytical methods

After mounting in epoxy, the sapphires were carefully cut by diamond wheel and repeatedly ground on 15 μm corundum powder until the mineral inclusions were exposed at the surface. Subsequent polishing utilized 6 μm, 3 μm and 1 μm diamond pastes, which resulted in a good quality polishing of the relatively soft inclusions.

The prepared samples were then carbon-coated for microprobe examination.

Electron microprobe (EMP). A LINK Energy Dispersive Spectrometer system (EDS) was used to identify and quantitatively analyse the unknown minerals. The acceleration voltage was set at 15 kV and the electron beam on the specimen was focused down to a 4–5 μm diameter spot. The beam current was calibrated on pure cobalt metal with a specimen current of 50 nA being used for routine quantitative analysis. Each spectrum was collected during a 100 s counting time. Any beam drift was corrected by remeasuring the beam current for 5 s immediately after the spectrum acquisition. The built-in ZAF correction program was used for quantitative calculation of element concentrations.

Proton microprobe (PMP). Minor and trace element contents in cobalt-rich spinels were analysed using the proton microprobe at the CSIRO Heavy Ion Analytical Facility Laboratory. The facility and the data reduction methods have been outlined by Griffin *et al.* (1988) and described in detail by Ryan *et al.* (1990). Briefly, a beam of 3 MeV protons, produced by a tandem electrostatic accelerator, was centred and focused onto the target using an electrostatic quadruplet lens. The beam spot on the sample surface was regulated to approximately 20–30 μm in diameter, with specimen currents around 10 nA. The X-rays produced by the bombardment were screened by Al- and Be- filters and then collected by a Si(Li) energy dispersive detector, followed by a now routine spectrum reduction procedure

TABLE 1. Representative probe analyses of the composite inclusion within sapphire (BP8).

Spot	3	8	4	7	5	12	13	14	16	#1	#2	#3	#4	#5
position	core	core	middle	middle	rim	rim	rim	rim		glass?	glass?	glass?	glass?	glass?
SiO_2	-	-	-	-	-	-	-	-	-	48.13	48.29	49.29	50.86	49.15
TiO_2	0.67	0.61	0.68	0.65	0.56	0.54	0.49	0.66	0.67	6.63	6.77	6.40	7.09	5.62
Al_2O_3	49.61	48.18	54.23	52.51	60.41	57.09	60.10	60.24	61.27	27.72	28.30	28.26	28.98	31.81
Cr_2O_3	11.57	12.28	8.01	8.67	3.69	5.82	3.27	3.79	-	-	-	-	-	-
FeO	9.55	9.67	8.94	9.68	8.98	8.86	8.79	8.64	8.96	3.34	3.31	2.36	2.50	2.07
MnO	-	-	-	-	-	-	-	-	-	-	-	-	-	-
MgO	6.04	6.42	6.06	6.11	6.41	6.18	6.42	6.56	6.89	0.69	1.03	0.40	0.54	0.40
CoO	22.38	22.84	21.82	21.79	19.79	20.72	20.25	20.25	21.92	0.83	1.13	0.72	0.83	0.46
NiO	-	0.50	-	-	-	0.58	-	0.57	-	-	-	-	-	-
CaO	-	-	-	-	-	-	-	-	-	0.24	0.32	0.28	0.27	0.23
Na_2O	-	-	-	-	-	-	-	-	-	2.79	3.22	2.73	2.48	1.94
K_2O	-	-	-	-	-	-	-	-	-	3.10	3.30	2.92	2.68	2.55
Total	99.82	100.50	99.74	99.41	99.84	99.79	99.32	100.70	99.71	93.47	95.67	93.36	96.23	94.23
Cations calculated on the basis of 4 oxygens														
Al	1.703	1.658	1.821	1.784	1.965	1.891	1.967	1.949	1.997					
Ti	0.015	0.013	0.015	0.014	0.012	0.011	0.010	0.014	0.014					
Cr	0.266	0.283	0.180	0.198	0.081	0.129	0.072	0.082	-					
Fe	0.233	0.236	0.213	0.233	0.207	0.208	0.204	0.198	0.207					
Mn	-	-	-	-	-	-	-	-	-					
Mg	0.262	0.279	0.257	0.263	0.264	0.259	0.266	0.269	0.284					
Co	0.523	0.535	0.499	0.504	0.438	0.467	0.451	0.446	0.486					
Ni	-	0.012	-	-	-	0.013	-	0.013	-					
ΣCAT	3.001	3.016	2.985	2.995	2.966	2.979	2.970	2.971	2.988					
Cr/(Cr+Al)	0.14	0.15	0.09	0.10	0.04	0.06	0.04	0.04	-					
ΣR^{3+}	1.984	1.954	2.016	1.996	2.057	2.032	2.049	2.045	2.011					
ΣR^{2+}	1.017	1.062	0.969	1.000	0.909	0.947	0.921	0.925	0.977					
X	0	−0.02	0.015	0.005	0.034	0.021	0.03	0.029	0.012					
X%	−0.03	−0.53	0.50	0.17	1.13	0.70	1.00	0.97	0.40					

Notes: 1. X denotes the number of vacancy, $X = 3 - \Sigma CAT$ (see text for discussion).
2. X% denotes the percentage of cation deficiency, $X\% = (1 - \Sigma CAT/3) \times 100\%$.
3. - not detected.

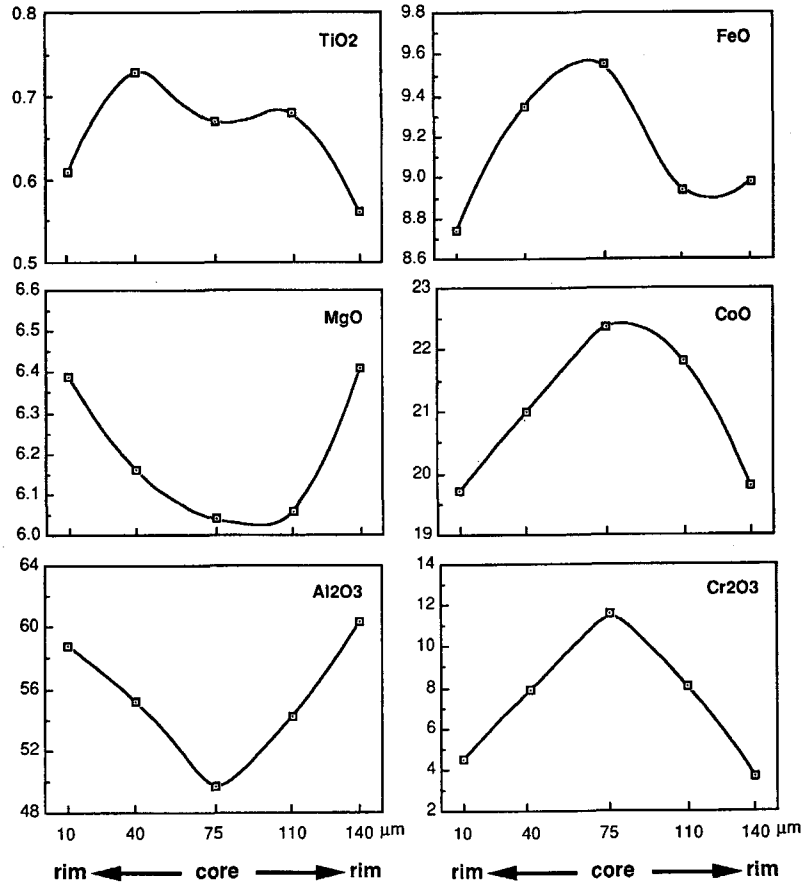

FIG. 3. The variations of oxide contents (wt.%) in the large spinel grain along section A–A′. The distance of analysed spots are relative to the bottom-left margin of the grain (Fig. 2*d*).

(Ryan *et al.*, 1990). The use of a Be filter enables analysis of elements with Z > (Cl). For analysis of the spinels reported here, a 200 μm Al filter was used to suppress the X-ray lines of all elements lighter than Co. The calculated element concentrations (PMP) have been normalised to the EMP values for Fe in order to reduce systematic errors and to minimise any bias in the measurement of accumulated charges on the sample surface.

The data obtained through such treatments have been compared with known standard values and demonstrated to be generally accurate to ±10% (Ryan *et al.*, 1990). The quoted analytical uncertainties are one standard deviation (1σ) derived from counting statistics. The minimum detection limit (MDL) for each element in an individual spectrum-acquisition process is also calculated from counting statistics, being at 99% confidence level. In this study, the element concentration values obtained for the cobalt-rich spinel are well above the MDL limits (20–60 times higher than MDL) with the exception of Mn. In the case of Mn, due to the high abundance of Co and Fe in the matrix, the peak overlaps of Co-*K*β–Mn-*K*α and Fe-*K*α–Mn-*K*β raise the detection limits for Mn (MDL: 130–170 p.p.m.); this hampers the precise determination of Mn contents. As a result, an uncertainty of up to 40% is given for the reported values. For a calculated concentration yield below MDL, the result is reported as < MDL.

Composition

Some representative EMP data on the composite inclusion are presented in Table 1. Strong zoning is

found across the large grain; Co and Cr are highest in the centre and Al highest along the margin, which is reflected by the gradual change of contrast from the centre to the margin in the BSE image (Fig. 2*c*). Without constraints on the Fe^{2+}/Fe^{3+} ratio, this analysis may be written to fit a spinel structural formula:

$(Co_{0.44-0.53}Mg_{0.26-0.28}Fe_{0.2-0.24}Ni_{<0.02})_{\Sigma 0.91-1.06}$
$(Al_{1.66-1.97}Cr_{0.06-0.28}Ti_{0.01-0.02})_{\Sigma 1.95-2.06}O_4$.

This cobalt-rich spinel, with significant Fe, Mg but minor Ni substitution in the structure, most closely resembles a previously reported cobalt-rich chromite, 'cochromite' (DeWaal, 1978), with a structural formula of

$(Ni_{0.5}Co_{0.22}Zn_{0.02}Mg_{0.05}Mn_{0.03}Fe^{2+}_{0.22})$-
$(Cr_{1.43}Al_{0.39}Fe^{3+}_{0.11}Ti_{0.03})O_4$.

Using the variation in Cr_2O_3 content, three zones may be recognized: central-, intermediate-

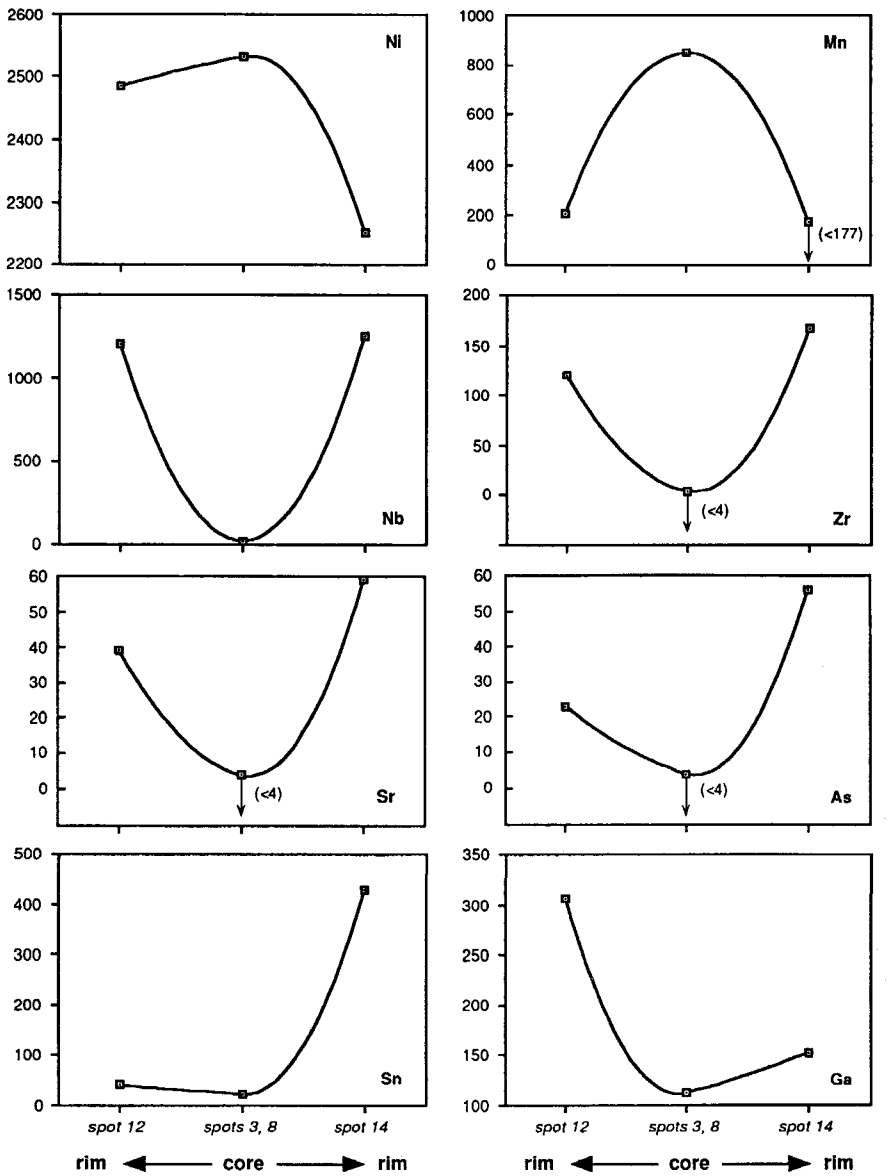

FIG. 4. The variations of minor and trace element contents (p.p.m.) in the cobalt-rich spinel

and marginal zones (Table 1 and Fig. 2*d*). The variations of individual oxides relative to the core of the grain are illustrated in Fig. 3. The Al_2O_3 content rises from 48.18% at the centre to 60.41% at the margin while CoO and Cr_2O_3 vary from 22.84 and 12.28% to 19.79 and 3.69% respectively. Although the absolute variations of other oxides are small from core to rim, they all display consistent changes corresponding to Al_2O_3, CoO and Cr_2O_3, i.e. FeO and TiO_2 decrease and MgO increases from the core to the rim. The compositions of small spinel crystals along the contact line show some similarities with those of large spinel rims, noticeably highest Al_2O_3 (61.27%) and MgO (6.89%) (No.16 in Table 1). However, the CoO contents of the small crystals are closer to the CoO range of the intermediate-zone of the large grain.

The centre and the margins of the large cobalt-rich spinel grain were also analysed by PMP; the data are presented in Table 2 and graphically illustrated in Fig. 4. A typical spectrum is shown in Fig. 5. It is not unexpected to see transition metal ions (Mn, Ni and Zn) and Ga in cobalt-rich spinel, but high Nb, Zr, Sn, As, Sr and Ag were also detected; the Nb content is as high as 1252 p.p.m. in the marginal zone while it is very low (24 p.p.m.) at the centre of the large spinel grain. The PMP values for Ni are lower than the EMP values, which are considered to be inaccurate due to the fact that they are very close to the EMP detection limits (Table 1). Mn and Ni, like other transition elements, decrease from core to rim of the cobalt-rich spinel while the other trace elements contents increase along with the the major elements Mg and Al. Nb and Zr are characteristic for this cobalt-rich spinel and probably reflect the chemical signature of the melt that produced the cobalt-rich spinel (see below).

The glassy matrix surrounding the cobalt-rich spinel inclusions, was analysed and proved to be a homogeneous silicate (Table 1). The totals of analyses are in the range of 93–96, indicating the presence of a volatile component, most probably H_2O. This glass is considered to have formed by the re-melting of a cobalt-rich spinel-bearing microassemblage when the enclosing sapphire was heated up by the hot basaltic magma that entrained the sapphire. The evidence for this interpretation is: (1) texturally, the small spinel crystals in the assemblage are distributed preferentially along the inclusion–sapphire contact,

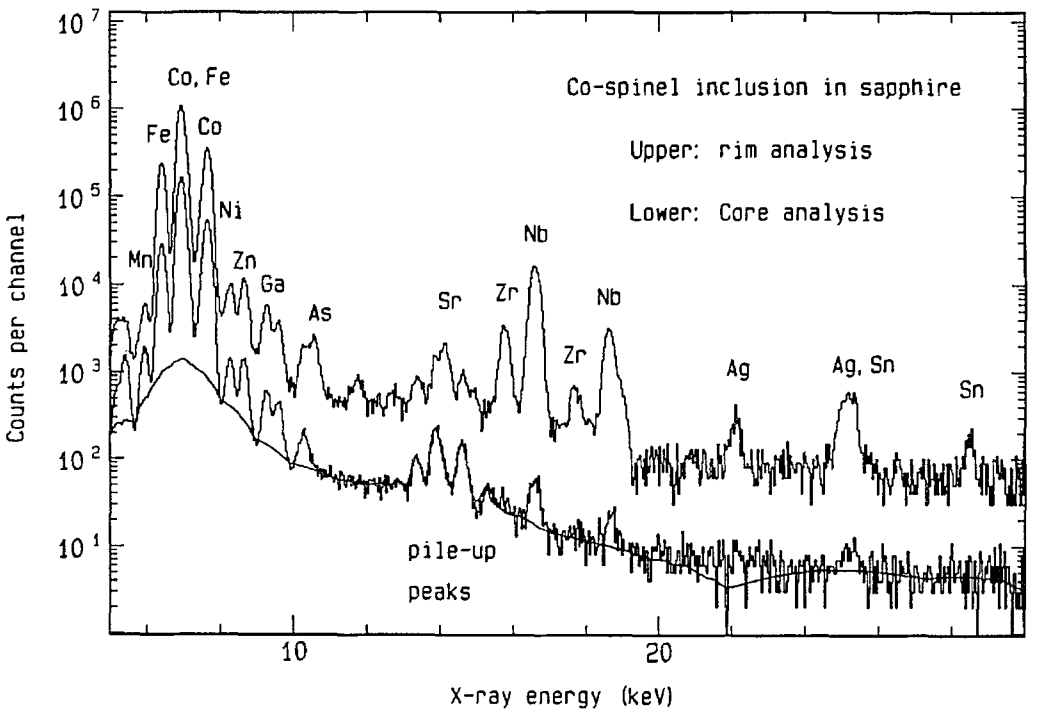

FIG. 5. A typical PIXE-spectrum of the cobalt-rich spinel.

indicating a post-inclusion arrangement; (2) compositionally, these small spinels are very similar to the rim of the large spinel grain, suggesting that they have been crystallized out of a relatively Cr-depleted and Al-enriched melt; this melt is readily available through partial melting of the original assemblage (a small portion of the cobalt-rich spinel + the 'unknown phase(s)'). The equivalent compositions of the 'unknown phase(s)' and the bulk assemblage were then calculated (Table 3). The significant amounts of K_2O and TiO_2 in the unknown phase(s) suggest the presence of phlogopite in the original assemblage.

Crystal chemistry

In the spinel structure, oxygen atoms are almost cubic close-packed to form a 3-D framework with cations occupying the octahedral and tetrahedral interstices. For a unit cell of 32 oxygens, all of the 16 octahedral sites and the 8 tetrahedral sites are filled with metal cations, resulting in a cation to oxygen ratio of 3:4, i.e. R_3O_4, where R represents cations with charges of 2+, 3+ or 4+. The extension of the unit cell forms an ideal spinel crystal leaving no vacant space in the structure. The numbers of each cation present in the cobalt-rich spinel crystal lattice, calculated on the basis of four oxygens, are given in Table 1.

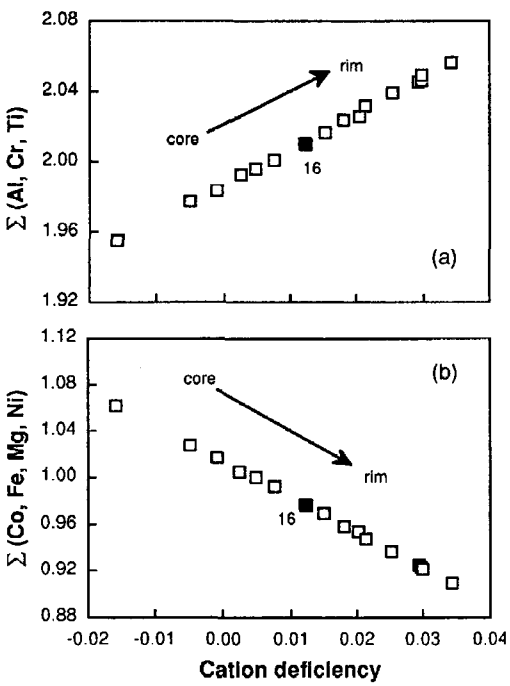

FIG. 6. The correlation between total cations and cation deficiency in cobalt-rich spinel. The analysis of a small spinel grain (No.16) is indicated for comparison.

Cation distribution. Assuming a normal spinel structure, the cobalt-rich spinel chemistry may be simplified into $(Co,Mg,Fe)(Al,Cr)_2O_4$. Around the core area (No. 3 and 8), the total R^{2+} (Co, Mg, Fe and Ni), denoted as ΣR^{2+}, is higher than the formula value 1.0 while the total R^{3+} (Al, Cr and Ti^{4+}), denoted as ΣR^{3+}, is lower than the theoretical formula value 2.0. The total number of cations (ΣCAT) is, however, equal to or higher than 3. On the other hand, the analysed spots from the intermediate zone towards the margin of the crystal show the opposite situation, i.e. $\Sigma R^{2+} < 1.0$, $\Sigma R^{3+} > 2.0$ and progressive cation deficiency ($\Sigma CAT < 3$) despite the fact that the scale of variation is small (Fig. 6). It is also noted from Fig. 6 that the degree of cation deficiency of the small spinel crystals along the contact line approaches that of the intermediate zone of the main spinel domain (also see Table 1).

Toriumi *et al.* (1978) synthesised $CoAl_2O_4$ with normal spinel structure while attempting to characterize the electron density distribution of 3*d* electrons (valence–electron) of the transition-metal Co in a tetrahedral field. The observed electron density deformation around atoms in $CoAl_2O_4$ suggests an effective charge of +1.5 for the Co atom. With no significant residual electron density present around the Al^{3+} ion, the authors concluded that the Co–O bond in $CoAl_2O_4$ was slightly covalent although it was still largely ionic. If this effective charge for Co is applicable to the cobalt-rich spinel, it is anticipated that, with all lattice sites filled, ΣR^{2+} will be slightly above the ideal value of 1.0 as the result of the normal formula calculation procedure. This fits well with the element distribution around the core position, also taking into account that a small amount of R^{2+} may occupy the octahedral site ('inverse' spinel; Wood *et al.*, 1986). Away from the core region, the progressive cation deficiency appears to be associated with the deviation of ΣR^{3+} and ΣR^{2+} from their formula values of 2.0 and 1.0 respectively (Fig. 6). Excess R^{3+} allocated to the tetrahedral site is, however, unable to compensate for the overall deviation of ΣCAT from the theoretical value 3.0. This may suggest the presence of a vacancy in the tetrahedral site within the cobalt-rich spinel structural lattice. Furthermore, a major element control of vacancy in the cobalt-rich spinel is implied by the fact that the increase of tetrahedral deficiency from core to rim of the large cobalt-rich spinel grain is accompanied by the steady changes in the

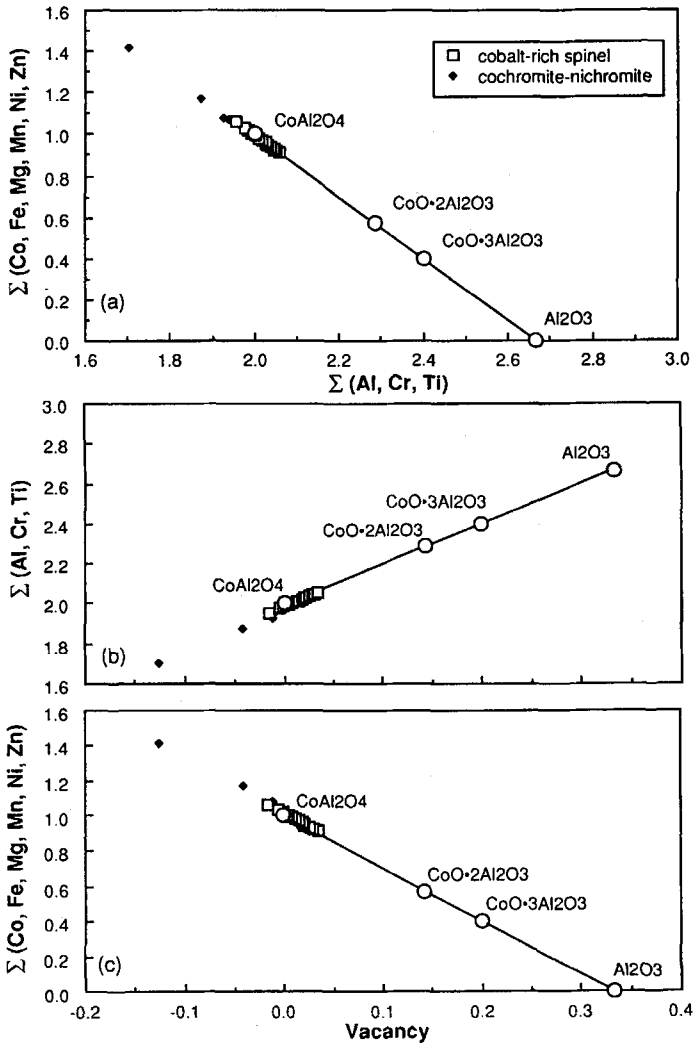

FIG. 7. The correlation between total cations and the number of vacancy in the cobalt-rich spinel structure, assuming that cation deficiency is equal to lattice vacancy. $CoO{\cdot}2Al_2O_3$ and $CoO{\cdot}3Al_2O_3$ are two hypothetical compounds. The tie-line between Al_2O_3 and $CoAl_2O_4$ is consistent with a substitution mechanism, $3Co^{2+} = 2Al^{3+} + {}^{[4]}\square$. Cochromite and nichromite data are taken from DeWaal (1978).

dominant major oxides Al_2O_3 and CoO, as discussed in the previous section (Fig. 3).

Figure 7 depicts the correlations between ΣR^{3+}, ΣR^{2+} and the assumed vacancy numbers per structural formula. It may not be a coincidence that the cobalt-rich spinel data fall onto the tie-line $CoAl_2O_4$–Al_2O_3 extrapolated to the previously reported cobalt-bearing spinels, cochromite and nichromite, on one end, and approaching the aluminium oxide (cubic γ-Al_2O_3?) on the other end (Fig. 7). This near perfect linear relationship is consistent with a vacancy involved substitution mechanism, $3Co^{2+} = 2Al^{3+} + {}^{[4]}\square$, i.e. the replacement of every three Co atoms by two Al atoms is accompanied by the formation of one vacancy in the spinel lattice to maintain charge balance. This is equivalent to an expression of $\{\square_x Co_{1-3x} Al_{2x}\}^{tet}\{Al_2\}^{oct}O_4$ or $\square_x Co_{1-3x}$-$Al_{2+2x}O_4$, with x representing the degree of substitution in spinel structure. It may be also

understood in such a way that the R^{3+} cation is unidirectionally 'inversed' into the tetrahedral site leaving some of the space unfilled. The higher the x index, the higher the degree of inversion of spinel. As a result, the total cation sum in a cobalt-rich spinel will be $\Sigma CAT = 3-x$. The $\Sigma R^{3+}/\Sigma R^{2+}$ ratio will depart from 2.0 but plus a factor of $8x$ after a first-order approximation. However, this substitution mechanism may be limited to a very small scale, cation deficiency being below 1.1% (Table 1). Notwithstanding the fact that EMP data have an uncertainty of about 1%, the systematic change of cation deficiency of the cobalt-rich spinel from core to rim, discussed above, supports the operation of such mechanism.

Solid solution. Using high-resolution NMR spectroscopy, Wood *et al.* (1986) were able to measure directly the distribution of Al between tetrahedral and octahedral sites of heated spinels (700–1425°C). Although the equilibrium inversion state did not survive quenching from temperatures above 900°C, the temperature dependence of spinel inversion was clearly observed. Their experimental results demonstrated that as temperature decreases, the atomic fraction of Al in the tetrahedral sites decreases, i.e. the cation distribution in spinel tends toward that of normal spinel at lower temperature. The degree of inversion [$x = Al^{tet}/(Al^{tet} + Al^{oct})$] for all heated samples is typically above 0.2, up to 0.4.

Jacob *et al.* (1986) experimentally determined the ion-exchange equilibrium in $CoCr_2O_4$–$CoAl_2O_4$ spinel solid solutions at 1100°C. Based on their thermodynamic mixing properties for the system $CoCr_2O_4$–$CoAl_2O_4$, the site occupancy in the cobalt-rich spinel that is mainly composed of these two members may be approximately estimated (Table I of Jacob *et al.*, 1986):

CORE ($X_{CoAl_2O_4} = 0.85$)
$[Co_{0.852}Al_{0.148}]^{tet}[Al_{1.552}Cr_{0.30}Co_{0.148}]^{oct}O_4$ and
RIM ($X_{CoAl_2O_4} \geqslant 0.95$)
$[Co_{0.844}Al_{0.156}]^{tet}[Al_{1.744}Cr_{0.10}Co_{0.156}]^{oct}O_4$.

The calculated results show a small degree of inversion (8–9% Al in tetrahedral sites), with all Cr distributed in the octahedral site. Such a low degree of inversion for the cobalt-rich spinel is in sharp contrast to that of heated spinels in several experimental studies (e.g. Schmocker and Waldner, 1976; Wood *et al.*, 1986), but similar to unheated natural samples of Schmocker and Waldner (1976). It may be suggested that the equilibrium temperature at which the cobalt-rich spinel was formed (or last equilibrated) had never been as high as 700°C. This also reinforces our judgement of this composite inclusion as the product of natural processes rather than that of laboratory heat-treatment, which is typically performed at temperatures above 1000°C.

On the basis of their experimental Gibbs free energy of mixing, Jacob *et al.* (1986) further predicted the appearance of a miscibility gap in the solid solution system $Co(Cr,Al)_2O_4$ at temperatures lower than 1100°C, with a critical solution temperature (Tc) of 549°C for the spinel of composition $X_{CoAl_2O_4} = 0.425$. It was suggested that two separate phases, $CoCr_2O_4$-based chromite ('ochromite') and $CoAl_2O_4$-based spinel ('cobalt-rich spinel'), may coexist below 550°C in suitable geochemical environments. As for the natural examples, since no exsolution phenomena are observed in both cobalt-rich spinel inclusions and the reported cochromite, a super-solvus crystallization is implied. Therefore, the equilibrium temperature for either cobalt-rich spinel or cochromite may be limited to above 350-400°C, applying the calculated solvus-curve of Jacob *et al.* (1986) (Fig. 8). This temperature estimate is not unrealistic when the geological occurrence of the cochromite phase is taken into account. Cochromite was initially found in a nickel-ore specimen in the Bon Accord nickel deposit of South Africa (DeWaal, 1978). It occurred, together with nichromite, in an unusual mineral assemblage of trevorite–liebenbergite–bunsenite as small grains and was considered to have formed by replacement of the early ore mineral chromite.

A note on petrogenesis

The only known spinels containing cobalt are some so-called 'cobalt-blue' spinels from Sri Lanka, but their cobalt contents are minor, typically less than 0.1% (Shigley and Stockton, 1984; Harder, 1986). There has been no previous report of a natural spinel with cobalt contents as high as that described in this study. The cobalt-rich spinel alone does not provide sufficient information with regard to its genesis. Its sole and unique occurrence (as a small inclusion in corundum) also prevents a detailed investigation. On the other hand, however, studies on sapphires from other alkalic basalt regions, e.g. the Inverell-Glen Innes region (NSW, Australia) and Wenchang (Hainan, China), have identified columbite, pyrochlore, albite, zircon and spinel as typical inclusions (Guo *et al.*, 1992*a*). This mineral assemblage suggests that complex magma mixing processes, probably involving an alkali-rich felsic melt and a silica-deficient carbonatite-type melt were involved in generating the inclusion–corundum associations (Guo *et al.*, 1992*a*,*b*). Bo Ploi sapphires are also derived from

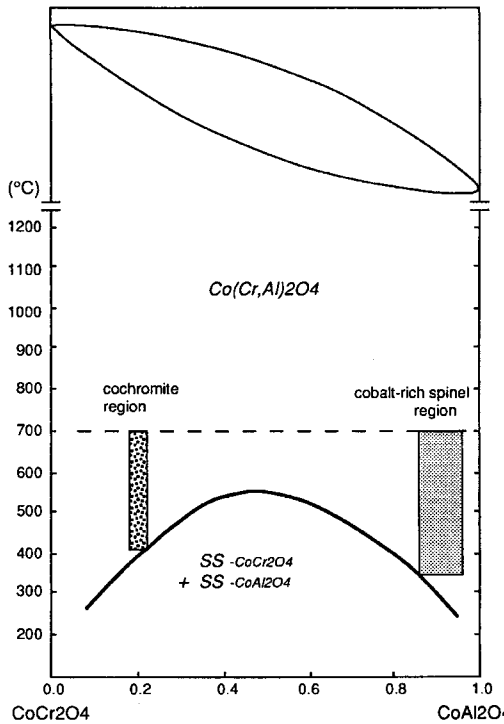

FIG. 8. An envisaged $CoCr_2O_4$–$CoAl_2O_4$ solid solution. According to Jacob *et al.* (1986), a continuous series of solid solution were obtained at the temperature of 1200°C, thus the liquidus–solidus loop is predicted to be above that temperature but without constraint. The (calculated) solvus-curve is also taken Jacob *et al.* (1986). The upper boundary for both cobalt-rich spinel and cochromite regions is derived from the order-disorder limit between heated and unheated natural spinels (see text for discussion).

basaltic rocks and considered to be the same origin as those from eastern Australia and eastern China.

In this study, because of the small number of samples available, we only find cobalt-rich spinel and albite as inclusions in the Bo Ploi sapphires. Together with the mineral inclusions identified by Gunawardene and Chawla (1984), we obtain an inclusion mineral suite: Co-rich spinel + albite + K-feldspar + Na-Mg-Al amphibole(?) + pyrrhotite. It is very likely that Nb-Ta oxide minerals such as columbite, Nb-rutile and pyrochlore may also be found as inclusion phases in Bo Ploi sapphires. Indeed, the high Nb concentration along the margin of the large cobalt-rich spinel grain (up to 1252 p.p.m.) does indicate a Nb-rich environment, which leads to the crystallization of Nb-Ta oxides. We therefore infer that the cobalt-rich spinel is the result of a complex magma mixing process in the lower crust. The evidence for and details of this process are outside the scope of this report and form the subject of a separate paper.

Acknowledgments

We wish to express our thanks to G & J Gems Pty Ltd (Sydney) for their generous supply of valuable sapphire samples and for providing some funding for this investigation. This work was also partially supported by the Australian Research Council through a small ARC Grant (Macquarie University) to SYO'R and WLG and a CSIRO/Macquarie collaborative grant. We thank Drs A. R. Ramsden and D. H. French for their assistance in taking BSE photographs using the CSIRO scanning electron microprobe. This study has been carried out while J. Guo was receiving a Macquarie University Postgraduate Research Award.

References

Barr, S. M. and MacDonald, A. S. (1978) Geochemistry and petrogenesis of late Cenozoic alkaline basalts of Thailand. *Geol. Soc. Malaysia Bull.*, **10**, 25–52.

Barr, S. M. and MacDonald, A. S. (1979) Palaeomagnetism, age, and geochemistry of the Denchai basalt, northern Thailand. *Earth Planet. Sci. Lett.*, **46**, 113–24.

Barr, S. M. and MacDonald, A. S. (1981) Geochemistry and geochronology of late Cenozoic basalts of southeast Asia: summary. *Geol. Soc. Amer. Bull.*, **92**, 508–12.

Bunopas, S. and Bunjitadulya, S. (1975) Geology of Amphoe Bo Ploi, North Kanchanaburi with special notes on the 'Kanchanaburi Series'. *J. Geol. Soc. Thai.*, **1**, 51–67.

DeWaal, S. A. (1978) Nickel minerals from Barberton, South Africa. VIII. The spinels cochromite and nichromite, and their significance to the origin of the Bon Accord nickel deposit. *Bull. Bur. Rech. Geol. Miniéres, Sec. II, Géol. Gites Minéraux*, no. 3, 225–23 (not seen; extracted from *Amer. Mineral.*, **65**, p. 811, 1980).

Griffin, W. L., Jaques, A. L., Sie, S. H., Ryan, C. G., Cousens, D. R. and Suter, G. F. (1988) Conditions of diamond growth: a proton microprobe study of inclusions in West Australian diamonds. *Contrib. Mineral. Petrol.*, **99**, 143–58.

Gübelin, E. J. and Koivula, J. I. (1986) *Photoatlas of Inclusions in Gemstones*. ABC Edition, Zurich.

Gunawardene, M. and Chawla, S. S. (1984) Sapphires from Kanchanaburi Province, Thailand. *J. Gemmol.*, **19**, 228–39.

Guo, J. F., O'Reilly, S. Y. and Griffin, W. L. (1992*a*) Origin of sapphire in eastern Australian basalts: Inferred from inclusion studies. *Abstracts of the 11th Australian Geological Convention, Ballarat, Victoria, Geological Society of Australia Abstracts No.* **32**, 219–20.

Guo, J. F., Wang, F. Q. and Yakoumelos, G. (1992*b*) Sapphires from Changle in Shandong Province, China. *Gems Gemol.*, **28**, 255–60.

Harder, von H. (1986) Natural cobalt-blue spinels from Ratnapura, Sri Lanka. *Neues Jahrb. Mineral., Mh.*, **3**, 97–100.

Jacob, K. T., Iyengar, G. N. K. and Kim, W. K. (1986) Spinel–corundum phase equilibria in the systems Mn–Cr–Al–O and Co–Cr–Al–O at 1373 K. *J. Amer. Ceram. Soc.*, **69**, 487–92.

Ryan, C. G., Cousens, D. R., Sie, S. H., Griffin, W. L., Suter, G. F. and Clayton, E. (1990) Quantitative PIXE microanalysis of geological material using the CSIRO proton microprobe. *Nucl. Instr. Meth.*, **B47**, 55–71.

Schmocker, U. and Waldner, F. (1976) The inversion parameter with respect to the space group of $MgAl_2O_4$ spinels. *J. Phys. C: Solid State Phys.*, **9**, L235–7.

Shigley, J. E. and Stockton, C. M. (1984) 'Cobalt-blue' gem spinels. *Gems Gemol.*, **20**, 34–41.

Toriumi, K., Ozima, M., Akaogi, M. and Saito, Y. (1978) Electron-density distribution in crystals of $CoAl_2O_4$. *Acta Crystallogr.*, **B34**, 1093–6.

Vichit, P., Vudhichativanich, S. and Hansawek, R. (1978) The distribution and some characteristics of corundum-bearing basalts in Thailand. *J. Geol. Soc. Thai.*, **3**, M4.1–M4.38.

Wood, B. J., Kirkpatrick, R. J. and Montez, B. (1986) Order–disorder phenomena in $MgAl_2O_4$ spinel. *Amer. Mineral.*, **71**, 999–1006.

[*Manuscript received 22 February 1993: revised 18 July 1993*]